Trend Deviation Analysis for Automated Detection of Defects in GPR Data for Road Condition Surveys

Alena Uus[1], Panos Liatsis[2], Gregory Slabaugh[1], Athanasios Anagnostis[3], Sam Roberts[4], Stephen Twist[4]

[1] City University London, Northampton Square, EC1V 0HB London, UK

[2] The Petroleum Institute, 2533 Abu Dhabi, UAE

[3] Center for Research and Technology – Hellas, GR 57001 Thessaloniki, Greece

[4] Met Geo Environmental Ltd., LS10 1SW Leeds, UK

alena.uus.2@city.ac.uk

***Abstract* - This paper presents a novel approach for automated detection of defects and structural changes in GPR data acquired in HMA (Hot Mix Asphalt) road surveys. Unlike the majority of the existing approaches for road GPR data processing that are mainly used for extraction of layer profile information, the proposed method focuses on automated identification of significant deviations in subsurface structure and material properties. It is based on detection of variations in intensity trends of longitudinal lines of interpolated B-scan that are characterized by deviation above the defined threshold. The corresponding outputs include mapped defects and deterioration areas together with the locations of detected changes in road structure design.**

***Keywords* – Road structural condition; Non-destructive testing; GPR processing; Automated defect detection**

I. Introduction

Ground penetrating radar (GPR) is an efficient and officially accepted non-destructive testing (NDT) tool in road condition surveys [2,3] for extraction and tracking of layer profile information required for structural condition inventory [4], identification of high void content areas or presence of moisture in subsurface layers [5,6], and detection of such defects as delaminations between layers or cracks [7-9]. It is also widely employed in concrete bridge deck inspection [10] for detection of rebar corrosion and delaminations.

Traditionally, 2D GPR data processing is based on detection of road layer interfaces and identification of changes and discontinuities related to variations in subsurface structure and material properties or the presence of defects and deterioration areas. The corresponding pre-processing methods generally include [11]: background removal, zero-offset correction, frequency and wavelet filtering. Next, various methods for layer interface detection and time-to-depth conversion procedure are used for road layer thickness assessment [12-13], while diffraction hyperbola detection methods are generally employed for structure mapping and identification of defects in concrete bridges [14]. Other reported methods for GPR data processing include deconvolution [15], independent component analysis [16], power curve analysis [17], and neural networks [18].

The majority of the existing GPR road data processing software systems mainly focus on automated detection and extraction of layer thickness and relative permittivity rather than detection of local defects. And although the presence of some of the defects will be reflected in the layer profile information, the corresponding analysis will require additional user input for mapping and interpretation. At the same time, early detection of deteriorations for planning of maintenance measures is essential for preservation of road structural condition. Furthermore, due to the large amount of GPR data collected during road surveys, there is a clear need for an automated solution for processing a GPR datastream to detect and map subsurface defects and structural changes for further analysis by an expert.

This paper describes a novel approach for processing and analysis of GPR data in HMA road surveys based on automated identification of significant trend deviations in subsurface structure and material properties independently of road layer construction design. The implemented method is a part of the post-processing software solution of RPB HealTec (Road Pavements & Bridge Deck Health Monitoring / Early Warning Using Advanced Inspection Technologies) (NDT) multisensor system for road condition surveys [1].

The proposed method is described in Section II followed by the analysis of the results, definition of the future research directions and conclusions in Section III and IV.

II. Proposed Method and Results

The summary of the steps of the proposed method for automated GPR data processing is presented in Figure 1. It includes B-scan pre-processing for enhancement of the subsurface structural features, which is then followed by the detection of interface reflection and interpolation of A-scans. Next, detection of the defects and deteriorations as well as road design changes is based on the extraction of longitudinal line trend derivatives and identification of the regions characterised by a critical “degree of deviation”, considered to be an indicator of significant changes in either structural or material properties. This approach is acceptable in the specific task of analysis of GPR data for a HMA road, since the layer structure of flexible road types is uniform and expected to be unchanging in the longitudinal direction. Next, the output in the form of a mapped trend deviation "alert" regions can be used in the decision support software in combination with the extracted layer profile information for maintenance planning [19].

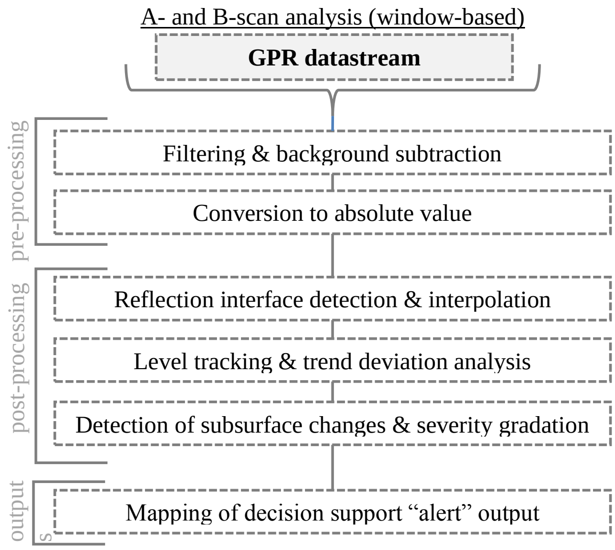

Figure 1. GPR data processing: proposed method

The performance of this method is demonstrated on an example of processing of a GPR road scan segment acquired during the preliminary field trials of 800 MHz air-coupled shielded MALA GPR antenna. The investigated road segment consists of the HMA surface-binder, base and subbase layers and was reported not to contain any severe road surface defects. However, the GPR B-scan section given in Figure 2 clearly shows the presence of subsurface defects and structural changes. In the highlighted region, all layers are affected and these changes are related to the presence of deteriorations in binder/base and base/subbase interfaces. There is also a pronounced disturbance in the surface reflection with higher intensity (reflection magnitude) corresponding to the material property changes.

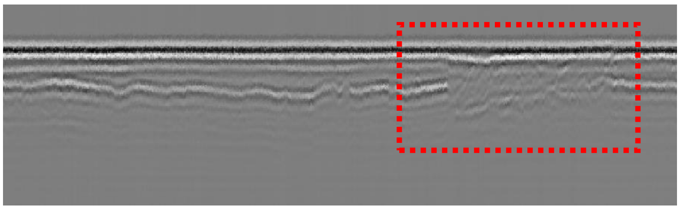

Figure 2. GPR processing example: original B-scan with highlighted defects

The software application based on this method was implemented in MATLAB R2014®. The GPR datastream processing is performed on the "window" basis with the B-scan window size (number of A-scans) set to a default value (e.g., 500) so that it fits within the specific display axes limits.

A. Preprocessing of GPR data

Following the performed 3px median filtering for noise removal and background subtraction, the A-scans are converted to absolute value in order conduct simultaneous analysis of both positive and negative components of the original received signal. Next, based on the detected reflection peaks, piecewise cubic interpolation is applied to every A-scan resulting in the continuous signal that comprises characteristics of all interface reflections. Figure 3 presents an example of a single A-scan pre-processing: (i) after filtering (A_F); (ii) after background subtraction based on morphological opening and conversion to absolute value (A_{BG}); (iii) and interpolation (A_I).

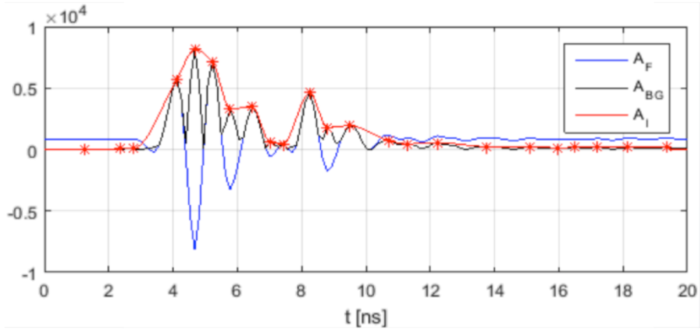

Figure 3. GPR processing example: pre-processing stage (A-scan)

The corresponding results for the investigated B-scan are shown in Figure 4. It can be clearly seen how the layer structure within the deteriorated region is enhanced after the performed background subtraction and conversion to absolute value (Figure 4.b). There is a significantly lower intensity of the reflection from the base-subbase layer interface caused by the change in the material properties as well as the structure deformation. The trend of the surface interface reflection is also affected with deviations in both structure and intensity.

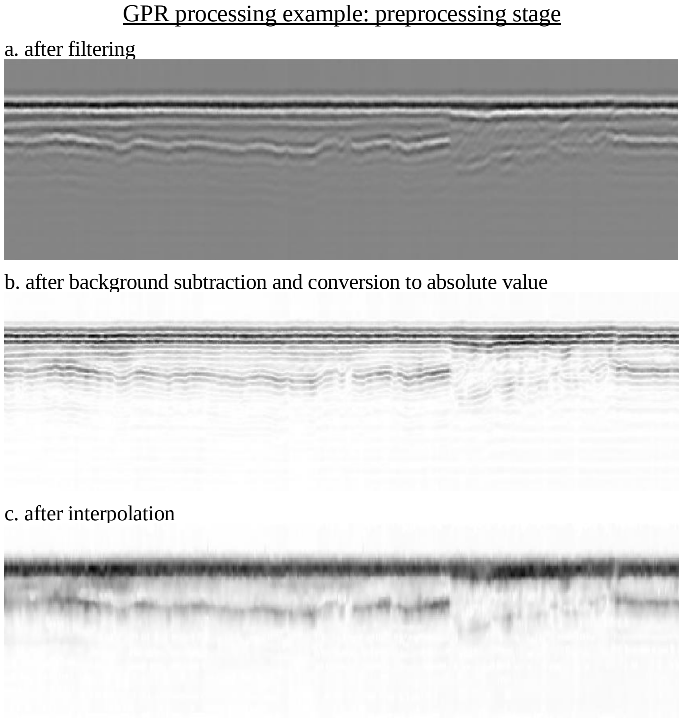

Figure 4. GPR processing example: pre-processing stage (B-scan)

The peak-based interpolation (Figure 4.c) provides the input for line-by-line trend analysis of the resulting B-scan. This novel approach has an advantage in comparison to the classical methods [11-13] that mainly focus on the analysis of detected reflection peaks only, which results in lower trend detection accuracy since the peak position and intensity magnitude can be disturbed due to various factors.

B. Analysis of GPR data

Next, the interpolated B-scans are analysed for the presence of significant trend deviations in the layer profiles corresponding to either the presence of deteriorations or changes in the road construction design. The expected output is the mapping of the locations of the detected deviations with “alert” flags. At first, the B-scan is automatically split into two regions corresponding to: (i) the HMA surface road layer and (ii) the base-subbase layers as shown in Figure 5. This procedure is performed based on the peak detection in the average A-scan. It has to be emphasized that this “division” into regions does not affect the accuracy of the defect detection and is mainly used in order to highlight and group defects with respect to their location and the number of regions can be increased.

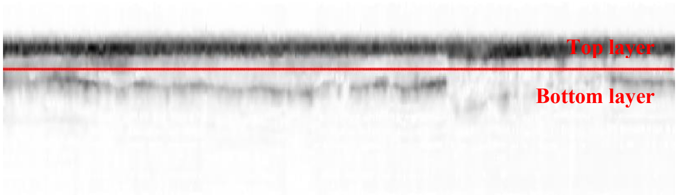

Figure 5. GPR processing example: division into layer regions

For each layer region, the deviations in the B-scan trends are tracked based on the analysis of the absolute derivative value of longitudinal line intensity levels. For instance, Figure 6.b shows the plotted intensity of the longitudinal lines of the top layer region. In this particular case, significant changes in the longitudinal level intensities can be observed in two regions (e.g., [75,125] and [325,375] A-scan sections). As mentioned above, these changes result from the combination of the structural and material property variations (e.g., trend shift and higher dielectric constant of the material).

<u>GPR processing example: analysis stage (top layer region)</u>

a. Top layer of the interpolated B-scan

b. Longitudinal line trend intensities

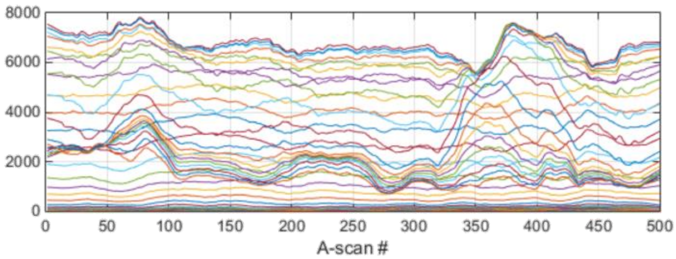

c. Modulus of the trend derivatives with detected peaks above the threshold

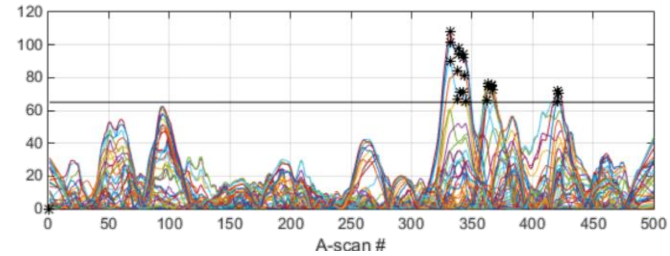

d. Detected critical trend deviations mapped on the original B-scan

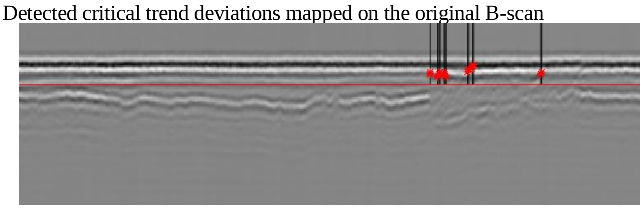

Figure 6. GPR processing example: analysis stage (top layer)

Next, the modulus of the derivative of the longitudinal trend lines is determined, providing a characterization of trend deviation. Significant defects or layer structure variations are detected using a sensitivity threshold, which is set to a default experimentally identified value and can be manually adjusted by the user. For instance, in this particular case (Figure 6.c), the sensitivity threshold is set to be 65 and the absolute derivative values above this threshold are considered to be “significant” (they are marked with black dots). Figure 6.d demonstrates the corresponding decision support output in the form of the original B-scan with mapped locations of the detected deviation “alert” flags.

The post-processing results for the bottom layer region are presented in Figure 7. Similarly, all areas characterised by the presence of significant trend deviations (e.g., A-scan regions: [50,75] [300,350] and [425,475]) in can be easily detected based on the analysis of longitudinal derivatives. In this example, the mapped detected “alert” flags (Figure 7.d) correspond to the changes of the base layer thickness and the presence of material deterioration, which can be also straightforwardly confirmed by visual interpretation.

<u>GPR processing example: analysis stage (bottom layer region)</u>

a. Bottom layer of the interpolated B-scan

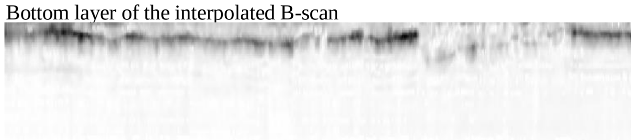

b. Longitudinal line trend intensities

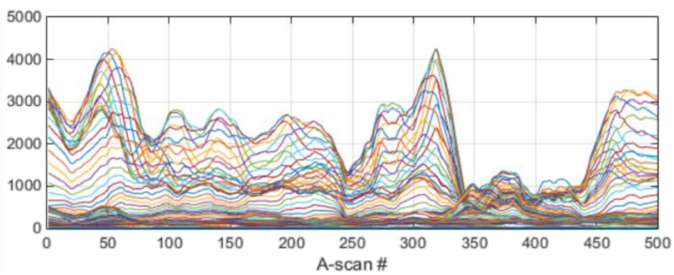

c. Modulus of the trend derivatives with detected peaks above the threshold

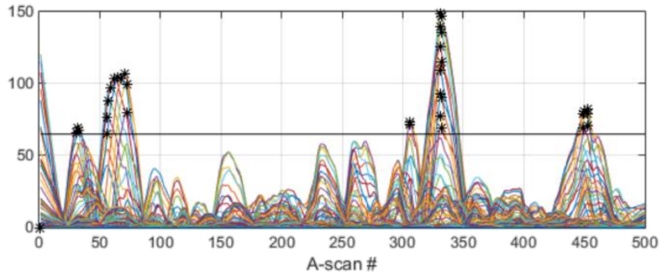

d. Detected critical trend deviations mapped on the original B-scan

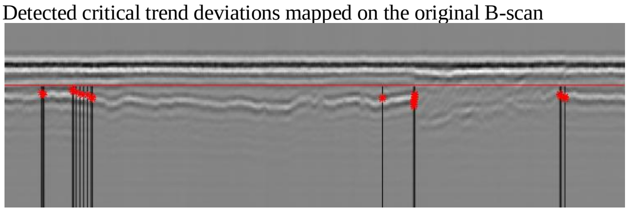

Figure 7. GPR processing example: analysis stage (bottom layer)

III. Discussion and Future Research Directions

In addition to the example demonstrated in the previous section, the outputs of processing of GPR scans of two road segments with the different degree of deterioration are given in Figure 8. In Case I, there is an evident presence of deviations in the layer interfaces as well as material property changes. The automated analysis successfully resulted in detection of a series of delaminations in the HMA/base layer interface, areas of higher reflection intensity in the surface layer, and variations in the base layer structure profile. On the other hand, in Case II (good structural condition), only one significant deviation "alert" was mapped, which corresponds to the change in the base layer thickness.

a. Case I: poor structural condition with structure and material changes

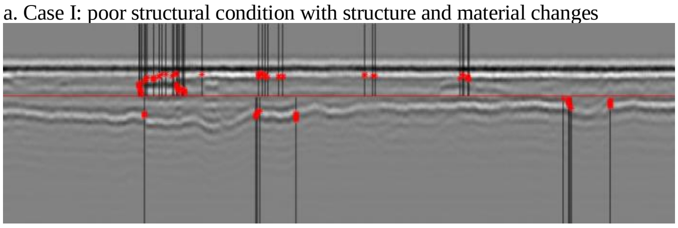

b. Case II: good structural condition without significant deterioration

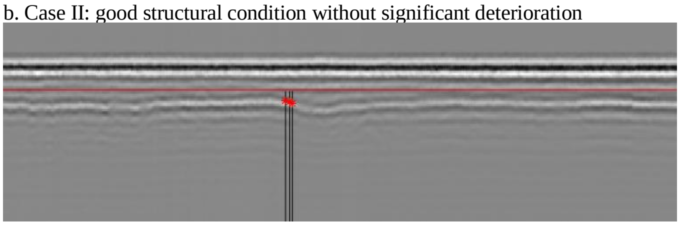

Figure 8. GPR processing results for two road segments with various degree of deterioration

In general, it can be concluded that the proposed method is effective in automated defection of subsurface structural changes and defects. However, as already mentioned, the defect detection sensitivity directly depends on the threshold corresponding to the degree of trend deviation. Therefore, the approach for definition of the threshold value requires further optimisation in order to avoid high numbers of false positive alarms. In theory, this value should mainly depend on the road structure and material properties and one of the proposed solutions is to incorporate machine learning based mechanism for automatic threshold adjustment. This will require analysis of the outcomes of the GPR field trials for various road construction design and subsurface defect cases with the corresponding user annotation and validation inputs. Other parameters that require investigation include the employed interpolation method and the degree of longitudinal trend smoothing.

Furthermore, the information output by the system can be potentially extended with the grading of defect severity based on the degree of trend change, analysis of reflection intensity value distribution or defect feature classification. The total number of "alerts" detected in one B-scan window can be used as a general characteristic of the road subsurface condition (or uniformity) and plotted along the entire length of the performed survey.

IV. Conclusions

This paper presented a novel approach for automated analysis of GPR data in HMA road surveys for detection and mapping of the critical "changes" in either structure or material properties of road layers such as the presence of subsurface defects, road construction design changes, presence of utilities, etc. This information can be used in road maintenance decision support systems in addition to the road layer profile characteristics extracted during routine GPR surveys.

One of the main advantages of the proposed solution is that it covers the entire range of possible subsurface changes rather than focusing on detection of specific defect features as well as being independent of the HMA road structure type.

The effectiveness of this method together with the optimal approaches for the processing parameter adjustment will be investigated based on the planned future GPR field trials, since it requires an extensive number of validated and annotated GPR data for statistical analysis.

Acknowledgment

The research leading to these results has received funding from the European Union's Seventh Framework Programme managed by REA-Research Executive Agency http://ec.europa.eu/research/rea ([FP7/2007-2013] [FP7/2007-2011]) under grant agreement No 606645 - RPB HealTec.

References

[1] FP7 RPB HealTec project. [Online]. Available: www.fp7-rpbhealtec.org . [Accessed: 20 Jan 2015].

[2] J. Hugenschmidt and P. Fürholz, "ATRAS – An automated GPR system for data acquisition and storage for roads and bridges," in 14th International Conference on Ground Penetrating Radar (GPR) June 4-8, 2012, Shanghai, China, 2012, pp. 448–453.

[3] T. Saarenketo and T. Scullion, "Road evaluation with ground penetrating radar," J. Appl. Geophys., vol. 43, pp. 119–138, 2000.

[4] I. L. Al-Qadi and S. Lahouar, “Measuring layer thicknesses with GPR – Theory to practice,” Constr. Build. Mater., vol. 19, pp. 763–772, 2005.

[5] J. Poikajärvi, K. Peisa, T. Herronen, P. O. Aursand, P. Maijala, and A. Narbro, “Nondestructive Testing and Evaluation GPR in road investigations – equipment tests and quality assurance of new asphalt pavement,” Nondestruct. Test. Eval., vol. 27, no. 3, pp. 293–303, 2012.

[6] D. Chen, F. Hong, W. Zhou, and P. Ying, “Estimating the hotmix asphalt air voids from ground penetrating radar,” NDT E Int., vol. 68, pp. 120–127, 2014.

[7] L. F. Walubita, T. Scullion, J. Leidy, and W. Liu, “Non-Destructive Testing Technologies: Application of the Ground Penetrating Radar (GPR) to Perpetual Pavements,” Road Mater. Pavement Des., vol. 10, no. 2, pp. 259–286, 2009.

[8] M. Celaya, “Evaluation of nondestructive technologies to assess presence and extent of delamination of hot mix asphalt airfield pavements,” PhD Thesis, Univ. Texas El Paso, 2011.

[9] L. Krysi and J. Sudyka, “GPR abilities in investigation of the pavement transversal cracks,” J. Appl. Geophys., vol. 97, pp. 27–36, 2013.

[10] A. M. Alani, M. Aboutalebi, and G. Kilic, “Applications of ground penetrating radar (GPR) in bridge deck monitoring and assessment,” J. Appl. Geophys., vol. 97, pp. 45–54, Oct. 2013.

[11] Sandmeier geophysical research, ReflexW Manual. [Online]. Available: www.sandmeier-geo.de/Download/reflexw_manual_a4_booklet.pdf . [Accessed: 20 Jan 2015].

[12] M. Solla, X. Nunez-Nieto, M. Varela-Gonzalez, J. MartInez-Sanchez, and P. Arias, “GPR for Road Inspection : Georeferencing and Efficient Approach to Data Processing and Visualization,” in 15th International Conference on Ground Penetrating Radar - GPR, June 30 - July 4, 2014, Brussels, Belgium, 2014, pp. 913–918.

[13] S. Lahouar and I. L. Al-Qadi, “Automatic detection of multiple pavement layers from GPR data,” NDT E Int., vol. 41, no. 2, pp. 69–81, 2008.

[14] Z. W. Wang, M. Zhou, G. Slabaugh, and T. Fang, “Automatic Detection of Bridge Deck Condition From Ground Penetrating Radar Images,” IEEE Trans. Autom. Sci. Eng., vol. 8, no. 3, pp. 633–640, 2011.

[15] I. Abdel-Qader, V. Krause, F. Abu-Amara, O. Abudayyeh, “Comparative Study of Deconvolution Algorithms for GPR Bridge Deck Imaging,” WSEAS Transactions on Signal Processing, vol. 10, pp. 20–31, 2014.

[16] F. Abu-amara, “An Automated Framework for Defect Detection in Concrete Bridge Decks Using Fractals and Independent Component Analysis,” PhD Thesis, Western Michigan University, 2010.

[17] S. Colagrande, D. Ranalli, and M. Tallini, “Ground Penetrating Radar Assessment of Flexible Road Pavement Degradation,” International Journal of Geophysics, vol. 11, 2011.

[18] Y. Cao, B. B. Guzina, and J. F. Labuz, “Pavement Evaluation Using Ground Penetrating Radar,.” 1. Report No. MN/RC 2008-10, Minnesota Department of Transportation, 2008.

[19] S. Miah, A. Uus, P. Liatsis, S. Roberts, S. Twist, M. Hovens, H. Godding, and G. Nardoni, “NDT Sensor Fusion: Optimisation of NDT Sensor Data Processing Strategies for Road Infrastructure Inspection,” in Universities’ Transport Study Group (UTSG) Conference, January 6-8 2016, Bristol, UK, 2016.